

## Shape-Selective Pathways in Methanol Conversion over Zeolite Catalysts

### INTRODUCTION

Mechanistic studies of the catalytic conversion of methanol over HZSM-5 (1, 2) have so far concentrated mostly on the intriguing problem of the first C-C bond formation (3, 4) and less attention has been paid to final mixtures. However, in this multistep reaction, precyclization pathways are clearly not intracrystalline diffusion controlled. Thus, olefin formation, growth, and cracking, unlike formation and distribution of the largest attainable molecules—naphthenics and aromatics—cannot reflect the special shape-selective properties of HZSM-5. The upper cutoff in product size over HZSM-5 presents a problem: HZSM-5 catalysts effective in the production of "gasoline" from methanol are non-*para*-selective providing, e.g., in the case of xylene, the thermodynamic equilibrium mixtures of positional isomers whereas under comparable conditions a highly *para*-selective HZSM-5 converts methanol mainly to small olefins. These facts are not realized straightforwardly. So is the fact that unlike the more widely open zeolites, such as HY and H-mordenite (HM), small-crystal ( $<1 \mu\text{m}$ ) HZSM-5 exhibits in methanol conversion and other transformations an astonishingly high resistance against deactivation. This apparently contradicts simple intracrystalline diffusion behavior according to which product growth above a certain critical molecular size soon causes practically irreversible zeolite pore-plugging thereby suppressing totally the catalytic activity. Large and/or modified HZSM-5 catalysts indeed reflect this property.

A plausible explanation to the above find-

ing is that the catalytic activity of HZSM-5 is a combined *para*-selective internal and non-*para*-selective external activity (5-7). Further, the external catalytic sites might be shape-selective (5) by virtue of their "nesting" properties (8, 9) which may be more pronounced than those of the large-pore zeolites. The alternative approach for shape-selectivity, based (for a given chemical system) solely on the length of the intracrystalline diffusion pathway (10) which determines the effectiveness factor ( $\eta$ ) for each product compound, appears to face serious drawbacks. It requires the assumption of primary product reentry into the crystal channels to explain lack of shape-selectivity and the estimated diffusion pathways leading to nonselective catalysis seem restricted to the order of magnitude of the cell parameter (a few nanometers). A recent theoretical study (11) shows the influence of combined external ( $\eta = 1$ ) and internal ( $\eta \leq 1$ ) catalytic activity in zeolites on the overall effectiveness factor. It may be interpreted as supporting the view that shape-selectivity, e.g., in HZSM-5, depends on the interplay between internal and external catalytic regime.

In this note we report on "final" product mixtures obtained in comparative batch experiments of methanol conversion over HZSM-5, HY, and HM and in comparative continuous-flow experiments using HZSM-5 samples of different properties. The results are believed to be in accord with the idea of shape-selective external activity ["nest effect" (8)] in HZSM-5.

### METHODS

Absolute methanol ( $\geq 99.6\%$ ) was obtained from Frutarom, Israel, and Argon

( $\geq 99.99\%$ ) from Oxygen Center, Israel. The catalysts used in this study were described in detail elsewhere (12). SC is a "standard" Mobil sample—a small-crystal ( $\approx 0.5 \mu\text{m}$ ) ZSM-5 in its  $\text{H}^+$ -form. LC-1 is a large-crystal ( $5\text{--}10 \mu\text{m}$ ) HZSM-5, and LC-2 is a large-crystal HZSM-5 containing a silica-boria amorphous phase. All the above HZSM-5 samples have Si/Al ratio of  $\approx 30$ .

Batch experiments were performed in a magnetically stirred 250-ml Parr-type autoclave at  $400^\circ\text{C}$ . In the case of SC, 1 g of catalyst was used with 20 ml methanol, while in the case of HY and HM, 5 g of preactivated catalyst was used with 50 ml methanol. During heating, a pressure buildup occurred (2–3 MPa). After 1 h, heating was stopped and the autoclave was allowed to cool down to room temperature. The excess gas pressure was then released before the autoclave was opened. With SC, the liquid product had a substantial organic layer above the aqueous phase. With HY and HM, only a large yellowish oil drop of organic liquid was obtained over the aqueous phase. The organic liquids were analyzed on Finnigan 4021 GC-MS instrument using a 30-m SE-54 capillary column (programming:  $45^\circ\text{C}$ , 5 min,  $4^\circ\text{C min}^{-1}$ ,  $200^\circ\text{C}$ ) and on Tracor 560 gas chromatograph equipped with an FID and a 3390A Hewlett-Packard integrator or a CSI supergrator-3A, using an OV-101 capillary column.

Flow experiments were performed under atmospheric pressure in a system and employing a procedure as described before (12). The condensed effluent was phase separated and each phase was weighted. The organic liquid was analyzed as before (12). The cold gas product was either trapped in a plastic bag for analysis or vented. Quantitative gas analyses were performed by wet test meter measurements. The amount of product gas was obtained by subtracting the amount of carrier gas from the total. For immediate periodic GC analyses, small gas samples (a few milliliters)

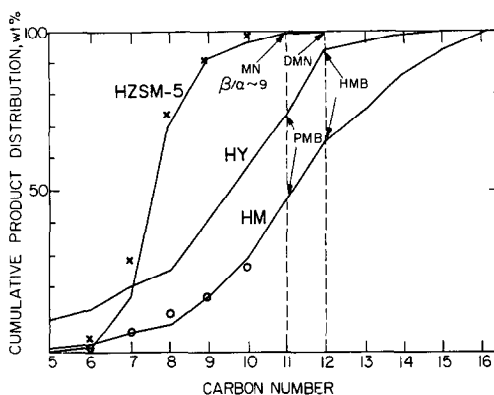


FIG. 1. Product distribution profile in batch experiments of methanol conversion over different zeolite catalysts. Symbols (x, o) represent corresponding literature results (Ref. (1)) of continuous-flow experiments ( $370^\circ\text{C}$ , 0.1 MPa, LHSV 1). MN, methyl naphthalene; DMN, dimethylnaphthalene.

were taken by a plastic gas syringe through a septum port installed in the gas tower far from its exit. Aqueous and gas samples were analyzed by gas chromatography over Porapak Q and Porapak QS columns. Under these analytic conditions no CO and  $\text{H}_2$  could be detected and their possible existence in the product gas was ignored.

## RESULTS

### 1. Batch Experiments with HZSM-5 (SC), HY, and HM

The batch mode, by providing a very long contact time between reactant and catalyst, allows to obtain approximately final reaction mixtures at 100% methanol conversion and thus assures "steady state." However, literature results with HZSM-5 and HM up to carbon number 10, obtained in the fixed-bed flow mode at a rather moderate contact time (1), appear in excellent agreement with our results thus establishing the meaning of the term final mixture in the present context. This is demonstrated in Fig. 1 in which results are plotted as cumulative product weight percent against carbon number. The significance of the present work is that it exceeds the  $\text{C}_{10}$  limit giving the entire product distribution, and

TABLE 1  
Largest Single Products (wt%) in Organic Layer  
Obtained in Batch Experiments of  
Methanol Conversion

	HZSM-5	HY	HM
Toluene	12.9		
Xylene	42.0 ( <i>m + p</i> ) 8.0 ( <i>o</i> )		
TMB	20.2	8.2	
TTMB	1.8 (1,2,4,5)	7.8	6.7
PMB		11.5	13.5
HMB		16.8	13.7

that it provides product structural identification as based on GC and GC-MS analysis. Since catalyst deactivation is not the result of chemical poisoning of catalytic sites but of pore-plugging and/or coke lay-down, even if the obtained mixtures could not be further converted because of catalyst deactivation, they nevertheless adequately reflect diffusional constraints owing to size limitation. As shown in Fig. 1, a transition region is observed in all cases, which is shallow for HY and HM and much sharper for HZSM-5. A parallel curving is detected for HY and HM but the plot of HM shifts ~1.5 carbon units toward a higher number and this may be explained by examining Tables 1 and 2. Table 1 presents the largest single products in the organic layer. For HZSM-5 (SC), the xylenes constitute 50% of total product, of which more than 85% are the mono-ring C<sub>7</sub>-C<sub>10</sub> aromatics. HM and HY give a quite different picture with a much wider product distribution. Pentamethylbenzene (PMB) and hexamethylbenzene (HMB) are far in excess to other products and constitute ~28% of the entire mixture while, in contrast, the amount of toluene and xylene (not shown) is only a few percent. Table 2 presents a comparison between HZSM-5 and HM, based on the GC-MS analysis, in terms of structural formulas of the main compounds found in the C<sub>10</sub>-C<sub>16</sub> range and the total number of products detected at each empiric formula. In

the case of HZSM-5, there is preference for elongated aromatics and the only products observed above C<sub>10</sub> are naphthalenics. In contrast, for HM most identified compounds up to C<sub>13</sub> were tetra-, penta-, and hexaalkylbenzenes, with methyl and ethyl as alkyl groups. However, from C<sub>13</sub> on, the product mixture apparently contained almost exclusively polymethylnaphthalenes and their hydro precursors. As seen in Fig. 1, these compounds constitute ca. one-third (!) of total product. With HY, the C<sub>13+</sub> fraction (of total organic liquid) is only ~0.06.

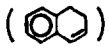
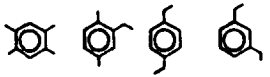


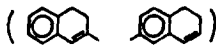
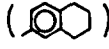
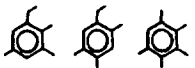
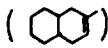
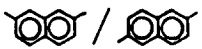
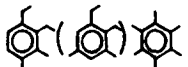

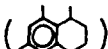
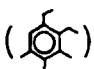
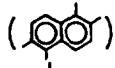
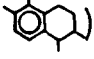
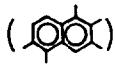
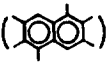
## 2. Continuous-Flow Experiments with HZSM-5 (SC, LC-1, and LC-2)

Extreme behaviors are observed for SC and LC-2 while LC-1 is a sort of midway between the two (Table 3). The differences between SC and LC-2 are easily seen in Figs. 2 and 3 presenting mass balance and hydrocarbon (HC) gas composition, respectively, as a function of time on stream (TOS). SC exhibits approximately constant activity during at least ~8 h (Fig. 2A) and a typical and constant butene/propane-rich gas mixture is obtained throughout the run (Fig. 3A). These results are similar to those reported in the literature (13). However, the effect of TOS in the case of LC-2 is very pronounced. Initially, the behavior is similar to that of SC but after ~2-3 h catalytic activity gradually declines as indicated by the amount of unreacted methanol, the production of dimethyl ether, and the decrease in organic liquid (Fig. 2B). Changes in the HC gas are also dramatic (Fig. 3B)—a strong decline in propane and butenes and a sharp increase in ethene and propene. Inhibition of the propene-to-propane reaction is, as expected, parallel to the suppression of aromatization, while the decrease in butenes may be at least partially correlated with the increase in ethene, hence attributed to a decline in ethene dimerization.

Table 3 compares catalysts SC, LC-1, and LC-2 in terms of product distribution in the organic liquid at two on-stream times. SC gives a constant product distribution

TABLE 2

Product Identification in the C<sub>10</sub>-C<sub>16</sub> Range of Hydrocarbon Mixtures Obtained in Batch Methanol Conversion Experiments

	<u>HZSM-5</u>		<u>HM</u>	
	<u>No. of products</u>	<u>Structural formula(e)<sup>a,b</sup></u>	<u>No. of products</u>	<u>Structural formula(e)<sup>a,b</sup></u>
C <sub>10</sub> H <sub>10</sub>	2	(  )		
C <sub>10</sub> H <sub>14</sub>	4		3	
C <sub>11</sub> H <sub>10</sub>	1			
C <sub>11</sub> H <sub>12</sub>	3	(  )		
C <sub>11</sub> H <sub>14</sub>	3	(  )		
C <sub>11</sub> H <sub>16</sub>			3	
C <sub>11</sub> H <sub>18</sub>			1	(  )
C <sub>12</sub> H <sub>12</sub>	1			
C <sub>12</sub> H <sub>18</sub>			3	
C <sub>13</sub> H <sub>14</sub>	2			
C <sub>13</sub> H <sub>18</sub>			1	(  )
C <sub>13</sub> H <sub>20</sub>			1	(  )
C <sub>14</sub> H <sub>16</sub>			3	(  )
C <sub>14</sub> H <sub>20</sub>			1	(  )
C <sub>15</sub> H <sub>18</sub>			4	(  )
C <sub>16</sub> H <sub>20</sub>			1	(  )

<sup>a</sup> Uncertain identifications are in parentheses.

<sup>b</sup> Only seemingly most probable isomers are presented.

TABLE 3  
Organic Liquid Analysis (wt%) in Methanol  
Conversion under Flow Conditions<sup>a</sup>

TOS (h):	1.75			7.75		
	SC	LC-1	LC-2	SC	LC-1	LC-2
Catalyst:						
Nonaromatics	13.5	12.4	16.3	12.3	22.1	32.2
Benzene	1.6	1.0	1.9	1.4	2.6	3.9
Toluene	11.4	11.6	14.9	11.1	7.3	2.5
Ethylbenzene	1.3	1.8	1.6	1.2	1.2	1.4
Xylene						
<i>p</i> -	9.3	21.1	32.0	9.8	22.5	34.9
<i>m</i> -	18.5	23.8	12.0	19.5	15.3	3.9
<i>o</i> -	9.2	9.9	4.0	9.5	5.9	1.4
Ethyltoluene						
<i>p</i> -	1.5	2.9	5.2	1.6	4.2	7.4
<i>m</i> -	3.3	4.1	3.5	3.3	4.2	1.3
<i>o</i> -	0.6	—	0.2	0.6	0.1	—
TMB						
1,2,4-	20.1	9.2	4.8	20.6	10.9	4.3
1,2,3-	1.4	0.4	0.6	0.6	0.6	0.8
Dimethylethylbenzene	2.9	0.7	1.0	3.1	0.8	1.6
1,2,4,5-TTMB	4.5	1.0	1.1	4.8	2.0	0.6
Others	0.9	0.1	0.9	0.6	0.3	3.8
Xylene isomer distribution (%)						
<i>p</i>	25.1	38.5	66.6	25.2	51.6	86.9
<i>m</i>	50.0	43.5	25.0	50.3	35.0	9.7
<i>o</i>	24.9	18.0	8.4	24.5	13.4	3.4

<sup>a</sup> For reaction conditions, see Fig. 2.

whereas LC-2 exhibits remarkable changes with time. The main trends are a relative increase in nonaromatics (mainly, olefins and naphthenes) and an increase in *para*-selectivity. While SC appears entirely non-*para*-selective, LC-2 exhibits a high initial *para*-selectivity, as reflected by both xylene

and ethyltoluene isomer distributions. *para*-Selectivity increases with TOS (in parallel with the decline in conversion, see Fig. 2B). With SC, the major aromatic product is 1,2,4-trimethylbenzene (1,2,4-TMB, ~20%) while in the case of LC-2 the main aromatic product is *p*-xylene. The amount of 1,2,4-TMB is ca. fourfold smaller with LC-2, compared to SC. Likewise, dimethylethylbenzene and 1,2,4,5-tetramethylbenzene (1,2,4,5-TTMB) are in much smaller concentrations in the liquid product of LC-2 than in that of SC. A similar change in the 1,2,4,5-TTMB content in methanol conversion mixtures was previously correlated with HZSM-5 crystal size (14). Table 3 thus confirms that with LC-2 there is considerably less tendency for aromatic polyalkylation while in the case of SC, substantial amounts of TMB and TTMB are produced with pronounced selectivity for the smallest isomers. PMB and HMB are not observed over HZSM-5 (any sample) even in traces.

#### DISCUSSION AND CONCLUSIONS

Shape-selectivity in zeolitic channels is attributed to the fact that molecules of different critical sizes at a size-range comparable with the channel cross-sectional dimensions diffuse in the intracrystalline space at different rates. It is further assumed that intracrystalline molecular diffusivities cor-

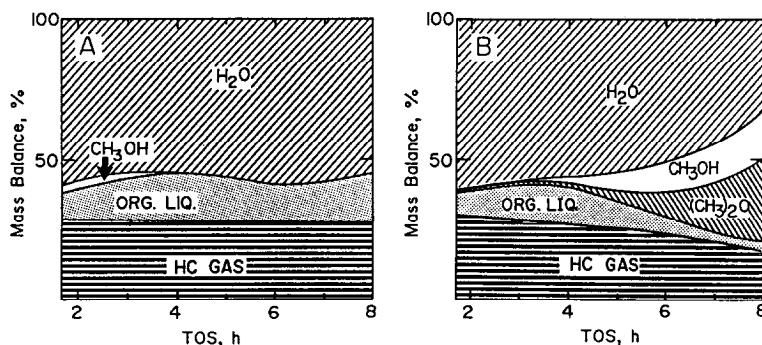


FIG. 2. Effect of time on stream on the efficiency of methanol conversion (370°C, 0.1 MPa, WHSV 1.5). (A) Catalyst, SC. (B) Catalyst, LC-2.

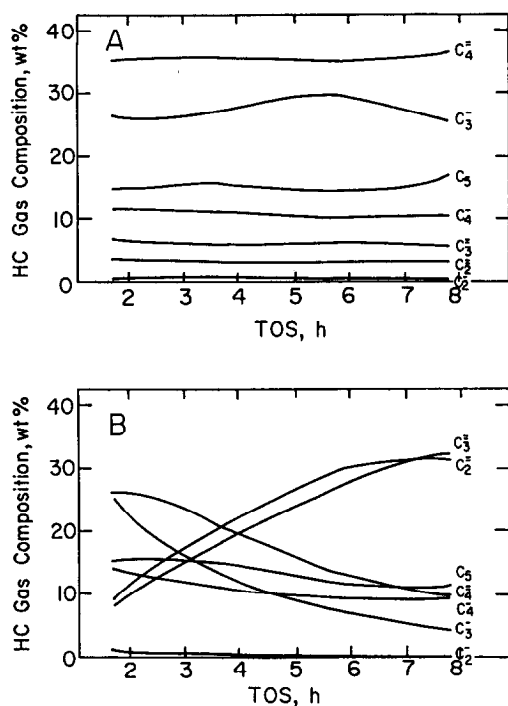


Fig. 3. Effect of time on stream on product HC gas distribution in methanol conversion (reaction conditions, as in Fig. 2). (A) Catalyst, SC. (B) Catalyst, LC-2.

relate with molecular critical size. Thus, one can interpret results of a shape-selective process in terms of critical sizes, using a proper molecular size scale (for example, the one employed in Ref. (5)), instead of diffusivities whose relevant values under the reaction conditions are usually impossible to obtain or at best, not readily available.

The results obtained in this study for HY and HM seem to correlate very well with the particular channel systems and the diffusional constraints imposed by them, both in terms of type of product and in terms of product distribution. The molecular size of the largest single products obtained, namely PMB and HMB, is in excellent agreement with the 12-ring channel dimension of both HY (7.4 Å) and HM (see below, Fig. 4). As expected, these channels do not cause any shape-selectivity in mono-ring aromatics below the critical size of PMB. The shift of the HM curve in Fig. 1,

with respect to the curve of HY, may in part reflect a higher tendency of HM to produce elongated double-ring compounds. This can be attributed to the fact that the 12-ring channels of mordenite are straight whereas those of zeolite Y have a zigzag array in which large and elongated molecules (e.g., polymethylnaphthalenes) may be caught by the so-called faujasite trap (15).

The medium-port 10-ring channel system of HZSM-5 imposes a shape-selective regime which is entirely different than that of HY and HM. We believe that this is best manifested in the case of LC-2, a highly *para*-selective catalyst (Table 3) whose catalytic activity drops considerably with TOS, as expected for intracrystalline zeolite catalysis. This catalyst is inefficient in the conversion of methanol to gasoline but after 8 h on stream it was found effective in methanol dehydration and production of

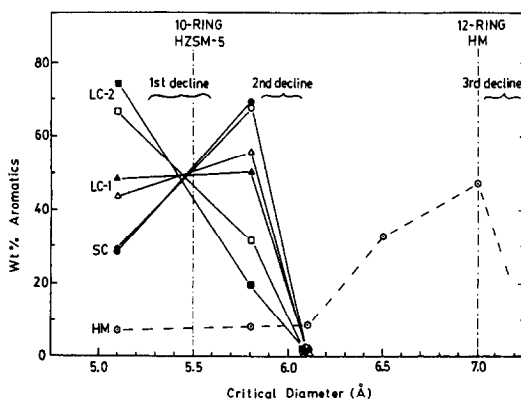


Fig. 4. Aromatics distribution as a function of critical molecular diameter for different zeolites at different TOS (open symbols, 1.75 h; closed symbols, 7.75 h, see Table 3). Because of the complexity of the mixture obtained with HM, only an estimate could be gained in this case (broken line). Zeolite opening values (nominal) are as given in W. M. Meier, and D. H. Olson, "Atlas of Zeolite Structure Types," Structure Commission of the International Zeolite Association, 1978. The molecular diameter scale is as used before (5): 5.1—benzene, toluene, ethylbenzene, *p*-xylene, *p*-ethyltoluene, and *p*-diethylbenzene; 5.8—*m*,*o*-xylene, *m*-ethyltoluene, 1,2,4-TMB, 1,2,4,5-TTMB, and 1,2,4-dimethylethylbenzene; 6.1—*o*-ethyltoluene, 1,2,3-TMB, and 1,2,3,4-TTMB; 6.5—PMB; 7.0—HMB, and polymethylnaphthalene (e.g., 1,2,3,5,6,7-hexamethylnaphthalene and precursors).

olefin-rich C<sub>2</sub>-C<sub>5</sub> gas mixtures. In contrast, SC is non-*para*-selective, highly efficient in gasoline production, and not affected by TOS at least during 8 h. While going from the silica-boria-modified LC-2 to the unmodified LC-1, then to the small-crystal SC, external surface size/activity is increased and the tortuosity of the intracrystalline diffusion pathway is decreased. Either one of these two effects may, in principle, explain shape-selectivity in HZSM-5, but we believe that the former effect provides a simpler and wider explanation to the experimental findings.

Figure 4 presents the organic liquid analysis for the different zeolite catalysts examined, both in the batch and in the flow experiments, as weight percent of product against critical molecular size. In the case of HZSM-5 catalysts, results are presented for the two on-stream times (Table 3), namely, 1.75 and 7.75 h. The picture revealed in Fig. 4 is self-explanatory. Of the three different declines in product content as a function of molecular size, two (i.e., the first and third) are easily associable with channel dimensions (i.e., cross-sectional free diameter of the 10- and 12-ring, respectively). For both LC-1 and SC, product distribution peaks in between the extremes, giving the second decline, the effect being most pronounced for SC with which almost no TOS dependence is noted. The interplay between the 5.1 and 5.8 points and the fact that regardless of the type of HZSM-5 catalyst and TOS, product amount corresponding to the 6.1 point is always almost insignificant, suggest that shape-selectivity in HZSM-5 is of a discontinuous nature. The second decline can, therefore, be assumed to result from surface or near-surface catalytic activity. The nesting principle (8) which applies to strongly curved surfaces allows to explain shape-selectivity of external HZSM-5 sites as well as their resistance against coking. Thus, according to Fig. 4, in an efficient methanol-to-gasoline process (e.g., using SC), the major gasoline product is attributable to external or near-external surface activity of HZSM-5. Certainly,

more rigorous research is required in order to establish this view.

#### ACKNOWLEDGMENT

We are indebted to C. S. Cheng of Mobil R&D Co. for providing us with a "standard" ZSM-5 sample (SC).

#### REFERENCES

1. Chang, C. D., "Hydrocarbons from Methanol." Marcel Dekker, New York 1983; *Catal. Rev. Sci. Eng.* **25**, 1 (1983).
2. Chang, C. D., and Silvestri, A. J., *CHEMTECH* **17**, 631 (1987).
3. Dessau, R. M., *J. Catal.* **99**, 111 (1986), and references therein.
4. van Hooff, J. H. C., van den Berg, J. P., Wolthuisen, J. P., and Volmer, A., in "Proceedings of the Sixth International Zeolite Conference, Reno, Nevada, July 10-15, 1983" (D. Olson and A. Bisio, Eds.), Butterworths, UK, p. 489; Mole, T., *J. Catal.* **84**, 423 (1983).
5. Fraenkel, D., Cherniavsky, M., and Levy, M., in "Proceedings, 8th International Congress on Catalysis, Berlin, 1984." Dechema, Frankfurt-am-Main, 1984, Vol. IV, p. 545.
6. Nayak, V. S., and Riekert, L., *Appl. Catal.* **23**, 403 (1986).
7. Kolboe, S., Larsen, M., and Anundskaas, A., in "Proceedings, 9th International Congress on Catalysis, Calgary, 1988" (M. J. Phillips and M. Ternan, Eds.), Vol. 1, p. 468. The Chemical Institute of Canada, Ottawa.
8. Derouane, E. G., *J. Catal.* **100**, 541 (1986).
9. Derouane, E. G., Andre, J.-M., and Lucas, A. A., *J. Catal.* **110**, 58 (1988).
10. Wei, J., *J. Catal.* **76**, 433 (1982).
11. Farcasiu, M., and Degnan, T. F., *Ind. Eng. Chem. Res.* **27**, 45 (1988).
12. Fraenkel, D., and Levy, M., *J. Catal.* **118**, 487 (1989).
13. Chang, C. D., and Silvestri, A. J., *J. Catal.* **47**, 249 (1977).
14. Pelrine, B. P., U.S. Patent 4,100,262 (1978).
15. Venuto, P. B., in "Molecular Sieve Zeolites - II," *Adv. Chem. Ser.* **102**, 260 (1971).

DAN FRAENKEL<sup>1</sup>  
MOSHE LEVY

*Department of Materials Research  
The Weizmann Institute of Science  
Rehovot, Israel*

*Received July 12, 1988; revised April 11, 1989*

<sup>1</sup> To whom correspondence should be addressed at University of Pittsburgh, Department of Chemical and Petroleum Engineering, 1249 Benedum Hall, Pittsburgh, PA 15261.